Acta Crystallographica Section D
Biological Crystallography
ISSN 0907-4449

Cool data: quantity AND quality

Elspeth Garman

Laboratory of Molecular Biophysics, Department of Biochemistry, University of Oxford, Oxford OX1 3QU, England

Correspondence e-mail: elspeth@biop.ox.ac.uk

Received 1 March 1999
Accepted 25 June 1999

The use of cryo-techniques in macromolecular crystallography has increased enormously over the last eight years and has become a vital part of modern X-ray data-collection methods. This paper presents some reasons for the rise in popularity of cryo-techniques and a brief outline of the basic methods, followed by a detailed discussion of factors to be considered when trying to optimize both the quantity and quality of the data collected. As more experimenters at synchrotrons observe significant radiation damage to crystals held near 100 K, the available options for further prolonging crystal lifetime and extending the techniques become worth investigating. Some possibilities and parameters to be considered are presented, although these must remain speculative until more experimental data are available.

1. Introduction

Cryocrystallography has come to the forefront as a pivotal tool in structural biology over the last eight years, driven largely by the great reduction in radiation damage to protein crystals during X-ray diffraction experiments at cryo-temperatures. At the last *CCP*4 Study Weekend on Data Collection in 1993, Steve Gamblin (Gamblin & Rodgers, 1993) summarized the cryo-techniques which have since been developed further in a number of laboratories (reviewed in Garman & Schneider, 1997; Rodgers, 1997). Six years ago, cryo-data collections were the exception rather than the rule. Today the situation is reversed; the techniques are currently being used by the majority of protein crystallographers and the advantages are now widely recognized.

In many ways, data collection with cryo-cooled crystals is much easier than with room-temperature samples, and some problems have disappeared altogether (*e.g.* crystal slippage). However, some aspects which did not previously merit consideration are now worth taking into account to ensure consistently high-quality data. Much of the subsequent work on the structure determination will be more straightforward if the best possible data are collected in the first place; if the original data are untrustworthy, they cannot be improved later on. In this paper, some measures for optimizing X-ray data quality are presented.

2. Why cool?

The main motivation behind the development of cryo-techniques was the observation (Low *et al.*, 1966; Haas & Rossmann, 1970) that radiation damage to protein crystals is greatly reduced at lower than room temperatures. In the early 1990s, radiation damage was becoming a limiting problem in

the full utilization of newly available synchrotron sources. Flash-cooling of crystals to near 100 K extends the crystal lifetime, making it effectively infinite on a home source and significantly prolonging it at the synchrotron.

Radiation damage is caused largely by 'primary' interactions between the molecules in the crystal and the beam. This energy is dissipated in at least two ways: it produces heat (thermal vibration of the molecules) and it provides the necessary energy to break bonds between the atoms in the molecules. The extent of this primary damage is dose-dependent.

There are two predominant mechanisms for producing reactive radicals: direct (*e.g.* damage to polypeptide) and indirect (reactive H* or OH* produced by destruction of a water molecule). Any thermal energy will allow the reactive products to diffuse through the crystal causing further destruction ('secondary' damage). This component of the radiation damage is time- and temperature-dependent.

At cryo-temperatures (around 100 K), the reactive products are immobilized in the crystal and do not cause extensive secondary damage in areas of the crystal which are not exposed to the beam. At room temperature, the reactive products diffuse and spread through the crystal, and this time-dependent secondary damage in addition to the primary dose-dependent part often destroys the crystal. Thus, cooling the samples for data collection significantly reduces radiation damage.

Because protein crystals can have a high water content, cooling them to around 100 K requires particular techniques. Work by Hope (1988) in extending small-molecule cryo-techniques for use with protein crystals prompted a number of researchers to undertake serious experimentation. Currently, the simplest and most generally used technique is the loop-mounting method of Teng, which has been developed further since it was originally reported (Teng, 1990). The crystal is first soaked for anything between 1 s and a few days (but usually around 3 min) in a so-called 'cryo-solution' (mother liquor plus an antifreeze agent; see §3). The crystal is then held by the surface tension of the cryo-solution across a loop made of thin (10–30 μm diameter) fibre (*e.g.* rayon, nylon, mohair, glass). It is immediately plunged into a cryogen such as gaseous nitrogen or liquid nitrogen, propane or ethane at temperatures around 100 K. The film of cryo-solution becomes solid and holds the crystal rigidly in the loop. The antifreeze in the cryo-solution and the rapid rate of freezing enable the crystal to be cooled to cryo-temperatures with no ordered ice formation; instead, a vitreous glass is formed which does not disrupt the crystal order or interfere with the diffraction.

A side benefit of cryo-techniques is that the loop-mounting method is a much gentler way of handling crystals than the glass or quartz capillary tubes used for room-temperature data collection. This factor enables very thin and/or small crystals to be used for structure determination. Thin crystals can be mounted in a large loop with the minimum of handling and it is possible to loop-mount without any physical contact with the crystal. For example, for the MIR structure determination of bovine cyclin A (Brown *et al.*, 1995), crystals of dimensions $100 \times 300 \times 5$ μm were successfully mounted in large loops for five derivative and two native data collections at synchrotron sources. Generally, small crystals suffer from fewer mechanical problems than larger ones and can be very successfully flash-cooled.

Owing to the prolonged lifetime of crystals held at cryo-temperatures, a whole data set can usually be collected from a single crystal. Systematic errors can thus be minimized, and this is very important for MAD experiments (Smith, 1991), where accurate data at three, four or even five incident X-ray

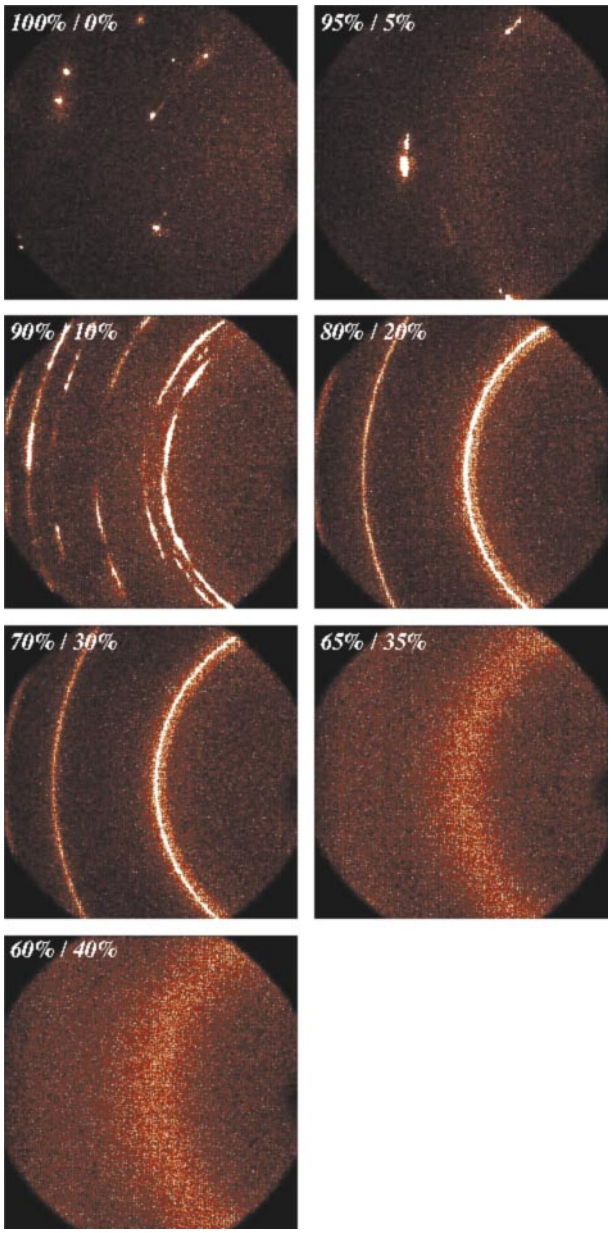

Figure 1
X-ray diffraction patterns of water/glycerol(*v*/*v*) mixes. The image from 60% water/40% glycerol shows that this solution is well cryoprotected, the scattering ring having similar shallow slopes on the high- and low-resolution sides (figure modified from Garman & Mitchell, 1996).

wavelengths are compared and the differences provide the phase information.

Another compelling reason for flash-cooling crystals is the potential to test them and then store them for later use in-house or at a synchrotron (Garman & Schneider, 1997; Rodgers, 1997). They can be frozen while in peak condition or stored if data collection has to be interrupted before completion. Once exposed, crystals stored in liquid nitrogen suffer minimum secondary radiation damage, unlike room-temperature crystals in capillaries, which will usually degrade with time once they have been subjected even briefly to an X-ray beam.

3. Basic loop-mounting technique

The first step in preparing to flash-cool a protein crystal is to find a suitable cryo-solution. This is usually the mother liquor with an antifreeze agent added (*e.g.* glycerol, ethylene glycol, MPD, light PEGs, sucrose) in sufficiently high concentration to prevent the formation of ordered ice and to promote vitrification of the sample. The mother liquor should not be diluted by the cryo-agent: the cryo-solution should be made up so that water in the mother liquor is replaced by cryo-agent (see §6.1). A test with the putative cryo-solution flash-cooled in the loop without the crystal will give the correct concentration needed. A clear film in the loop is a necessary but not sufficient criterion: a diffraction image should always be taken to check for diffuse rings from ice crystallites. Fig. 1 shows images from water/glycerol mixtures containing increasing concentrations of glycerol. Satisfactory cryo-protection is afforded by addition of 40% glycerol; the diffuse scattering ring has a similar slope on the high- and low-resolution sides (Garman & Mitchell, 1996). If a crystal and mother liquor are transferred to the cryo-solution, the cryo-solution will be diluted, and thus it is wise to increase the cryo-agent concentration by 2–5% as a safety margin in order to take the dilution into account.

Next, the crystal is introduced into the cryo-solution, broadly in three alternative ways. For most crystals, the easiest option, which is usually satisfactory, is to transfer the sample from its growing drop straight into the final concentration of cryo-solution and leave it for between 30 s and 4 min. It must be emphasized that this soak time is rather empirical; a longer soak allows more time for equilibration but prolongs the time during which the cryo-solution can degrade the crystal, whereas a short soak does not achieve osmotic equilibration of the crystal but minimizes the degradation time. Times between 0.5 s (crystal dragged through cryo-solution) and several days have been used successfully, and there is a huge variation in soaking times used in different laboratories practising cryo-crystallography. Sequential soaks in increasing concentrations can also be used; these lessen the osmotic shock to the crystal (see §5.3 and §6.4).

Cryoprotectant agents can also be dialysed into the crystal, and this method often succeeds where soaking has failed (*e.g.* Nagata *et al.*, 1996). However, the ideal case, which minimizes the crystal handling, is where the crystals are grown in a mother liquor which is already adequately cryoprotected. In fact, some such crystal screens are now commercially available. An account of this approach is given in Garman (1999).

Most laboratories are now equipped to allow rapid mounting of the crystal in the loop from the cryo-solution onto the goniostat; a typical arrangement is shown in Fig. 2. The volume of cryo-solvent around the crystal can be minimized by lifting the loop out of the cryo-solvent so that its plane is perpendicular to the surface of the drop. Further practical details of the method can be found in Garman & Schneider (1997) and Rodgers (1997).

4. Quantity

As already mentioned, the potential now exists to collect all the required/desired data from a single crystal. In terms of quantity of data, what is desirable?

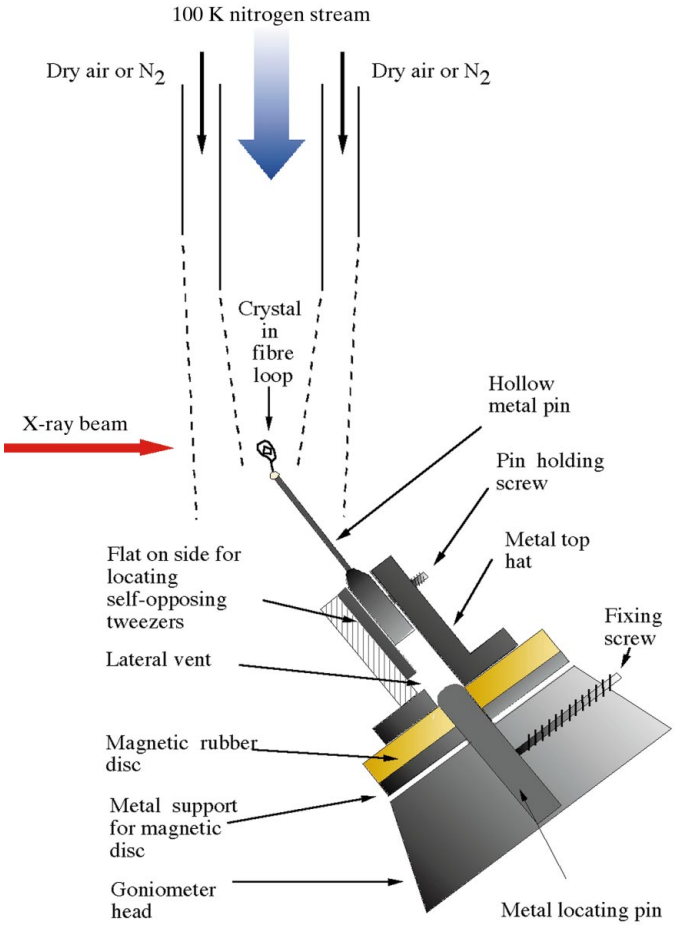

Figure 2
A typical experimental arrangement for a cryocrystallographic data collection. A magnetic rubber disc is pierced with a stainless steel pin, the top of which is rounded and the bottom of which fits into the hole in the goniometer head. The magnet must be strong enough to make a rigid connection, but weak enough to allow the experimenter fine control of the top hat, which is fabricated from a magnetic metal such as stainless steel or nickel. (Figure reproduced from Garman & Schneider, 1997.)

4.1. Completeness

Whatever the purpose of the data collection, the data are likely to be much more useful if they are complete; *i.e.* the number of unique reflections collected in each resolution shell is at least 95% of the theoretical maximum number. With the recent advent of reliable data-collection strategy software (Messerschmidt & Pflugrath, 1987; Kabsch, 1988; Leslie, 1996; Noble, 1996; Ravelli *et al.*, 1997), this is now routinely possible.

The first image is autoindexed to find the unit cell and possible space group, and the experimental parameters are refined to obtain satisfactory agreement between the predicted and actual spot positions. Some data-strategy software programmes (*e.g.* the 'strategy' option in *MOSFLM*; Leslie, 1996) can be used at this stage, whereas others (*e.g. PREDICT*; Noble, 1996) require prior integration of a single image. This output is then used by the strategy software to either calculate the completeness obtained for a total oscillation angle specified by the experimenter, or to find the oscillation range necessary for a desired completeness and then to advise on the optimum starting angle for the data collection. An example of the output from such a calculation is shown in Fig. 3 for a crystal in point group 321 for a 60° total oscillation angle. It can be seen that the overall completeness is in antiphase with the redundancy (number of times the intensity of each unique reflection is measured). If the anomolous signal is required for phasing, the optimum starting angle is not necessarily the same as for optimizing the overall completeness.

Before starting a data collection, it is advisable to collect an image 90° away from the first test image to check for correct centring and for anisotropic disorder (see Garman, 1993) in the crystal.

For low-symmetry space groups, the crystal is sometimes in an unfavourable orientation and it is hard to obtain complete data owing to geometric constraints on the experiment, especially when using only a single-axis goniostat. If a removeable arc goniometer (see Garman & Schneider, 1997) is used for crystal storage, the arm can be attached so that the crystal can be conveniently moved around to access new parts of reciprocal space. Care must be taken to avoid collisions between the arc and the collimator during the data collection. Another possible solution is to glue a piece of narrow-gauge wire onto the loop-mounting pin (David, 1999) and then stick the loop to this, as shown in Fig. 4. After the first sweep of data has been collected, the wire can be bent with plastic tweezers or another non-heat-conducting material tool in order to place the crystal in a new orientation with respect to the beam. Care must be taken not to displace the crystal too far from the centre of the cold gas stream during the wire bending; an iterative procedure of bending and centring is usually necessary.

4.2. Redundancy

A higher redundancy or 'multiplicity', where each unique reflection is measured multiple times, will result in more accurate data even though $R(I)_{\rm sym}$ might become larger, where $R(I)_{\rm sym}$ is

$$R(I)_{\rm sym} = \sum |I - \langle I \rangle| / \sum |\langle I \rangle|,$$

and $\langle I \rangle$ is the mean intensity of a set of equivalent reflections. In the extreme case, where most unique reflections are measured only once, $R(I)_{\rm sym}$ for the data set will be lower than if each were measured four or five times, but the latter data would be more accurate and thus more reliable. Software now available can again be used to give an indication of the average redundancy which will be collected for a specified angular sweep. It is important to check this for low-symmetry space groups, since in some unfortunate orientations the redundancy is likely to be very low.

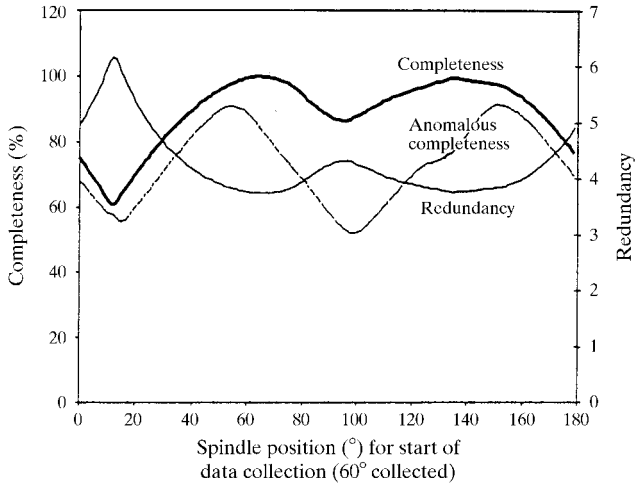

Figure 3
The results of running *PREDICT* (Noble, 1996) for a crystal of point group *P*321 to find the overall completeness, anomalous completeness and redundancy for a 60° sweep starting at different φ angles.

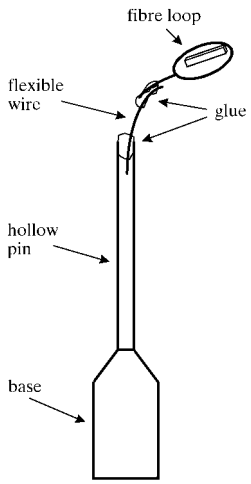

Figure 4
A cryo-loop design for crystals of a low-symmetry space group. A piece of narrow-gauge wire is inserted between the mounting pin and fibre loop. The wire can then be bent to different positions (taking care that the crystal remains in the cold nitrogen stream at all times) for access to different parts of reciprocal space.

4.3. Higher resolution

Cryo-cooled crystals in general diffract to higher resolution than the same crystals at room temperature for two main reasons. Radiation damage tends first to be evident in the higher range order (which gives the higher resolution diffraction) and thermal vibrations are in general lower for structures determined at 100 K, giving enhanced diffraction intensity at higher resolution (see §7.3.2 for two examples). In addition, sometimes the soak in the cryo-solution, especially PEGs, causes dehydration which results in increased order (e.gs. Schick & Jurnak, 1994; Esnouf *et al.*, 1998).

It can be tempting to try and obtain the highest resolution possible, but if the higher resolution data are collected, a smaller oscillation angle per image will be required to avoid overlapping reflections at higher resolutions. This implies more images and thus more time will be needed for the data collection. Additionally, the low-resolution reflections may be overloaded (see §5.2) at the exposure times needed to give adequate statistics for the faint high-resolution data and so one or more low-resolution passes may be necessary, which will take even more time. All this should be considered at the stage of deciding on the data-collection parameters (Mitchell *et al.*, 1999).

4.4. Crystal storage

Since crystals can be stored for later re-use, more data can be collected at a future date if necessary. The techniques for storing crystals (Garman & Schneider, 1997; Rodgers, 1997; Parkin & Hope, 1998) are still evolving and it is hoped they will become more foolproof in the next few years; currently the success rate is rather variable and the technique is not as reliable as it might be. During the next few years, service crystallography is likely to become a feature of synchrotron-radiation sites, so it will be even more important for retrieval of cryo-cooled crystals to be as reproducible as possible.

5. Quality

Cryo-cooling also provides the opportunity to optimize the quality of the data which are collected, since the prolonged crystal lifetime allows more time for the experiment. Paradoxically, the flash-cooling technique can also introduce features which compromise the data quality, such as increased mosaicity and ice diffraction. Experimental parameters can be adjusted to improve data quality by considering the factors discussed below.

5.1. Overloads

Overloaded reflections are those where some individual pixels have so many counts that the detector response is no longer linear, *i.e.* the number of counts in the pixel is not a reliable measure of the number of X-rays arriving at that position on the detector. These reflections should be rejected by using the appropriate switch in the processing software, since intense inaccurate low-resolution data can have a serious detrimental effect on the resulting electron density. Data with overloads rejected will be less complete at low resolution than at high resolution (see Fig. 5), but low-resolution data are vital for structure solution and also for obtaining interpretable good-quality electron-density maps. It is thus very important that reliable low-resolution data are collected by either performing a second lower resolution and lower exposure time (or dose) sweep or by reducing the exposure time per image of the original sweep until there are no overloaded reflections. The latter strategy may be incompatible with collecting reasonable $I/\sigma(I)$ at high resolution (see §5.4). The experimenter should check locally for the number of counts per pixel above which a particular detector is known to have a non-linear response.

In the event that a significant fraction of the low-resolution reflections are overloaded and no low-resolution pass was collected owing to instrumental or other problems, information on the low-resolution reflections can be obtained by fitting their tails to a model peak shape and extrapolating this peak height to obtain a measure of the reflection intensity (*e.g.* in *MOSFLM*, use the input line 'profile fitted'). Although this method will have a larger error than a properly measured experimental intensity, it is much better than having no measure at all. An example of this situation is shown in Fig. 5. Data processed with the overloads rejected gave $R(I)_{\rm sym}$ of 6.6% and a completeness of 96.7% overall but only 32–72% for the 15–5.5 Å data, and resulted in uninterpretable electron density for the cell-cycle protein CDK2 with an inhibitor bound. With fitted profiles for the overloaded reflections, $R(I)_{\rm sym}$ increased to 7.7%, the data were 99.7% complete overall (838 more unique reflections) and the resulting electron density was interpretable and very clean. Note that in *SCALEPACK* overloads can be included at the scaling stage with the 'include overloads' keywords.

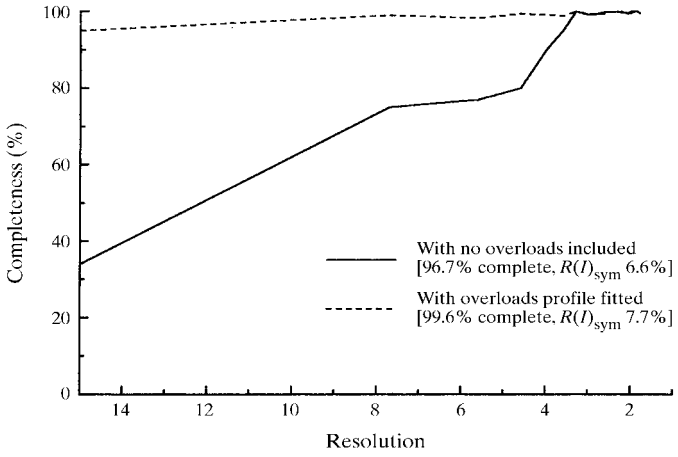

Figure 5
Completeness *versus* resolution for a crystal of CDK2 cell-cycle protein soaked in an inhibitor solution. Data were collected at BW7B, EMBL, Hamburg and serious detector problems prevented the collection of a low-resolution data set. The plot shows the effect of rejecting overloaded reflections and also of profile-fitting them. Data with the overloads rejected were very incomplete at low resolution and electron-density maps calculated from them were uninterpretable. With profile-fitted overloads, the more complete data set resulted in good electron density.

5.2. Overlaps

It is wise to minimize the number of overlapping reflections, since they will be rejected by the integration software, thus causing the data to have lower completeness. Since the resolution limit is in general higher for flash-cooled crystals, more care must be taken to avoid collecting overlapped reflections. For a two-dimensional data collection, the maximum oscillation angle per image, $\Delta\varphi_m$, to minimize overlaps is

$$\Delta\varphi_m = \frac{\text{maximum resolution of data (Å)}}{\text{maximum primitive cell (Å)}} \times \frac{360}{2\pi} - \text{mosaicity (}^\circ\text{)},$$

e.g. if collecting 1.8 Å data with a maximum primitive cell edge of 200 Å, a $\Delta\varphi_m$ of 0.5° would be appropriate, assuming zero mosaicity. The above formula shows that in order to minimize the number of overlaps for a given $\Delta\varphi$, the mosaicity also has to be minimized (see below).

5.3. Mosaicity

A common observation is that the mosaic spread of cryo-cooled crystals tends to be higher than that of the same crystal at room temperature. Increased mosaicity adversely affects the data quality since it increases the number of overlaps (see §5.2), it decreases the signal-to-noise ratio of a reflection as the reflection is spread over a larger volume of reciprocal space and for two-dimensional data collection it decreases the ratio of fully to partially recorded reflections (see Fig. 6). The decrease in signal-to-noise ratio with increasing mosaicity usually means that if the mosaicity is minimized, the diffraction limit is maximized (see Mitchell & Garman, 1994, where this was shown for crystals of phosphorylase *b*).

Mosaic spread can be increased by any handling of the crystals, which should thus be minimized. By investing some time into exploring different cryo-conditions, cryo-solutions and soaking methods, it should be possible to reproduce room-temperature mosaicity in most cases. Rocking curves can most easily be collected and investigated on an electronic area detector (*e.g.* a CCD-based detector or a multiwire) where three-dimensional data collection is time-efficient and thus three-dimensional profiles of reflections can be obtained to give an accurate measure of the mosaicity.

Sequential soaking in increasing concentrations of cryo-solution, rather than putting the crystal into the final concentration, can reduce the mosaicity. During a sequential soak, both the handling of the crystal and the severity of the osmotic shock to it of the 5 or 10% increases in the concentrations of cryo-agent can be lessened by the following simple measure. The crystal and mother liquor are left in the same microbridge or soaking well and 10% cryosolution is pipetted onto them, the drop is agitated with the pipette end without touching the crystal and then some of the liquid (say 10 µl) is removed. 10 µl of the 10% solution is now added again, mixed, 10 µl removed, 10 µl of the 20% cryo-solution added, mixed and so on until the desired concentration of cryo-solution is reached. The resulting increase in cryo-solution concentration is illustrated in Fig. 7. For crystals of the 42 kDa neur-

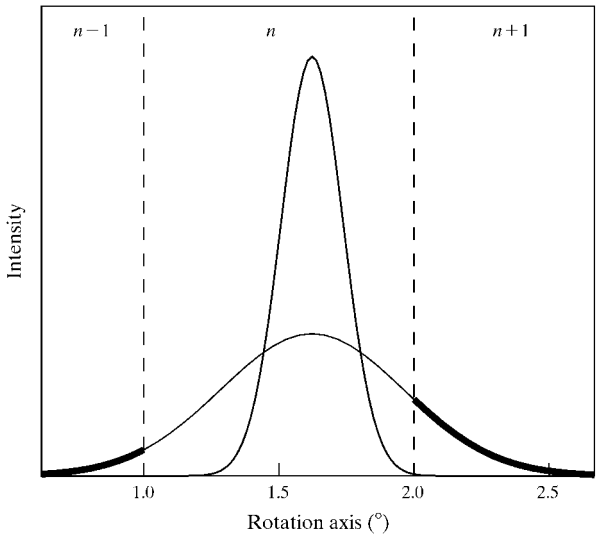

Figure 6
The profile of a high and low mosaic spread reflection of equal total intensity as a function of φ angle. For a low mosaic spread reflection, a 1° oscillation image will encompass the whole reflection, which will thus be 'fully recorded'. For a reflection with larger mosaic spread, the same reflection intensity is detected over three consecutive 1° images, and is 'partially recorded' on the $(n-1)$th, nth and $(n+1)$th images. To obtain the full reflection intensity, these images must be scaled together after integration, resulting in higher errors (σs) on the measurements.

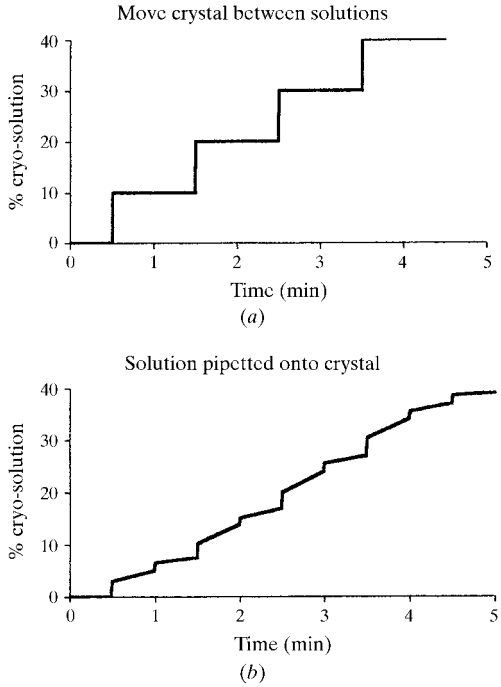

Figure 7
Concentration of cryo-solution *versus* time for (*a*) a sequential 1 min soak in each of 10, 20, 30 and 40% solutions, transferring the crystal between solutions, and (*b*) leaving the crystal in the same place in a 10 µl drop of mother liquor and pipetting 10 µl of 10% cryo-solution onto it, mixing, waiting 30 s, removing 10 µl, adding another 10 µl of 10%, mixing, waiting 30 s, removing 10 µl, adding 10 µl of 20% and so on. In (*b*) the crystal is subjected to more gradual osmotic shock as the concentration of cryo-solution is increased.

aminidase from *Salmonella typhimurium* (STNA), for which some time was spent experimenting with cryo-protocols to optimize diffraction, this method resulted in routinely obtaining resolutions better than 1.0 Å at the synchrotron, whereas moving the crystal between microbridges during the sequential soak gave resolutions worse than 1.0 Å and non-sequential soaking gave resolutions of around 1.3 Å.

Several factors can affect the mosaic spread during the actual cooling procedure. Swift transfer from the drop to the cryogen is desirable, since the crystal surface can dehydrate while travelling through the air. Placing the microscope as close as possible to the cryogen, as well as practizing the transfer on several 'dry runs' beforehand, minimizes the transfer time.

The rate of crystal cooling is another important factor: in general, the faster the cooling the lower the resulting mosaic spread. Since the rate of cooling is critically dependent on the crystal surface-to-volume (S/V) ratio, those with larger S/V tend to cool better than those with smaller S/V (*cf.* insects having high S/V which do not survive in the winter). However, a balance must be struck between the desirable increase in diffracting power of high-volume crystals and the undesirable increase in mosaicity observed when flash-cooling them.

The choice of cryogen can also affect the rate of cooling and hence the mosaic spread (see §6.2). Crystal annealing can be used to reduce the mosaic spread (see §6.5).

5.4. $I/\sigma(I)$ and $R(I)_{\rm sym}$

For good quality data, the average $I/\sigma(I)$ of the high-resolution reflections should be monitored during the experiment and kept at a significant value. Dauter (1997) has suggested that as a rough guide, more than 50% of the data in the highest resolution shell should advisably have $I/\sigma(I) > 2$. He has also suggested that data might be cut for shells having an $R(I)_{\rm sym}$ value above 30%, although higher values might be acceptable for higher symmetry space groups and lower values for $P1$. However, some experimenters prefer to include all data. Some statistics for a high-resolution data collection on STNA are shown in Fig. 8. It can be seen that $\langle I/\sigma(I)\rangle$ drops below 2 at around 1.04 Å and that $R(I)_{\rm sym}$ rises above 50% at 1.03 Å. In this case, data were cut at 1.05 Å, since the data quality becomes significantly worse beyond this value. Including all data to 0.97 Å in the refinement did not appear to improve the electron-density maps or give the positions of any additional H atoms.

5.5. Orientation of the loop

Depending on the space group of the crystal, there may be several choices given by the data-collection strategy program for the optimum starting angle of the oscillation sweep. For instance, in the example shown in Fig. 3, the experimenter could choose to collect 60° of data starting at 60° or at 130°. One of these options might be much better than the other in terms of the relative orientation of the beam and the cryo-loop; it should be possible to avoid hitting the crystal parallel to the plane of the loop, where intensity will be lost and fibre diffraction from the loop will possibly be observed.

Some protein crystals exhibit rather asymmetric diffraction limits, and again a judicious choice of data sweep can optimize the data which are actually collected. For example, crystals of viral neuraminidase subtype N8 diffract to 1.7 Å in the *ab* plane and 3.0 Å in the *c* direction.

5.6. Heavy-atom/substrate soaks

When performing heavy-atom/substrate/inhibitor soaks, the heavy atom/substrate/inhibitor should be added to the cryo-solution, even if the cryo-soak is short. Competitive binding can sometimes occur between the cryoprotecting agent and the desired substrate, so that the electron-density map will disappointingly reveal a molecule of the cryoprotective agent in the catalytic/active site. A new, non-competitive cryoprotecting agent will have to be found [*e.g.* for phosphorylase *b*, glycerol was observed to be a competitive inhibitor (Gregoriou *et al.*, 1998) and MPD was subsequently used successfully]. A recent systematic study of the effects of different cryoprotective agents on the activity and structure of phosphorylase *b* (Tsitsanou *et al.*, 1999) showed that the most active form of the enzyme is stabilized to different extents by some agents (MPD, PEGs of various sizes and DMSO). The DMSO and MPD did not induce conformational changes in the X-ray structure and did not bind to the catalytic site.

Bound cryo-agent molecules are also commonly observed in electron density calculated from cryo-data sets (*e.g.* six glycerols in STNA; Garman *et al.*, 1996) and these bound molecules can affect the observed structure of the macromolecule. The crystallographer must thus be aware of the possibility that conformational changes and alterations in ligand binding can be induced by the introduction of cryoprotective agents.

Non-isomorphism, even between native data sets, can be more pronounced when using cryo-techniques for two reasons.

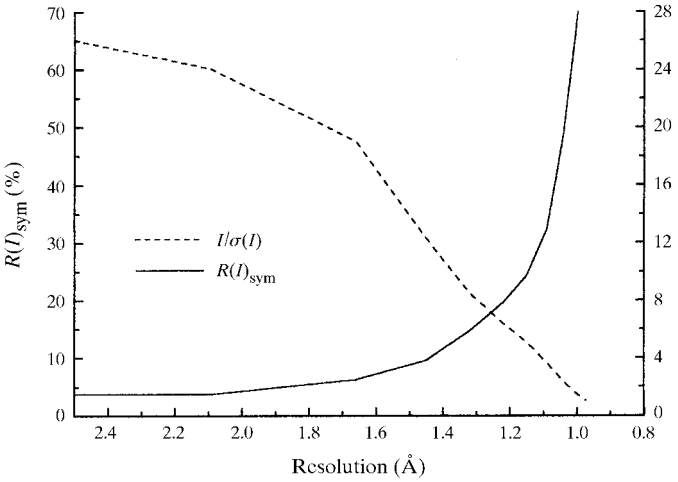

Figure 8
Data statistics for a high-resolution data collection at BW7B, EMBL, Hamburg, from a crystal of the 42 kDa enzyme *S. typhimurium* neuraminidase (STNA). Data were cut at a resolution of 1.05 Å, since $\langle I/\sigma(I)\rangle$ was below 2 and $R(I)_{\rm sym}$ was above 50% beyond this.

The first is that some cryoprotecting agents can dehydrate crystals and cause shrinkage. The second is that the cooling procedure itself causes shrinkage owing to the decrease in volume between water in the sample and the vitreous ice (glass) formed on flash-cooling. The degree of shrinkage seems to depend on the solvent content of the crystal and the exact cooling protocol used. Therefore, to increase the chance of isomorphous data, identical procedures should be followed [soak times, crystal size (if possible), cryo-solution concentrations, cryogen temperature]. If practicable, the same human being should flash-cool the crystals, since then idiosyncracies of procedure will be the same.

Flash-cooling has enabled experimenters to start using krypton and xenon routinely in the search for heavy-atom derivatives (Soltis *et al.*, 1997; Sauer *et al.*, 1997). A crystal suspended in its cryo-solution in a loop is bathed in gas at up to 1.5 MPa pressure for about 10 min. The main prerequisite is that the crystal should be stable in the cryo-solution for 10 min at room temperature. Several laboratories have built devices to facilitate the technique and two of these are available commercially (from MSC and from Oxford Cryosystems).

5.7. Ice

In spite of efforts to avoid ice formation (see Garman & Schneider, 1997, for detailed discussion), some ice may gradually accumulate on the sample during the experiment. This will be evident on the diffraction pattern, either as diffuse rings, sharp rings or individual reflections (see Fig. 1). Ice can be carefully removed with a small artist's brush or with an acupuncture needle attached to a non-heat-conducting rod. Alternatively, a little liquid nitrogen can be poured onto the loop.

However, if there are ice features on the images, their effect on the data quality can be minimized during data processing. If the software allows, the ice diffraction is best masked out before integration rather than at the scaling stage. For instance, in *MOSFLM*, the input line 'resolution exclude 3.87 3.93' would remove the 3.90 Å ice ring. In *DENZO* (Otwinowski & Minor, 1997), the command 'reject X' can be used, where X is the proportion of background pixels which must satisfy the constraints imposed by the software on the slope and uniformity of the background. The default value of X is 0.75, and it can be increased sequentially in small steps (it is a sensitive parameter) to 0.76, 0.77 *etc.* until no spots are predicted on the ice rings, as these spots usually have a high and irregular background and thus do not give accurate intensity values. The same software commands can be used to mask out reflections from salt crystals, which occasionally form in high-salt cryo-solutions during the transfer of the loop to the goniostat.

Monitoring the images as they are collected and removing ice if it forms is the best way to minimize the problem. Other foreign bodies can sometimes cause shadows on the diffraction image and can be dealt with if the quality of the images is being continually checked. For instance, flying insects can become frozen onto the end of the cryonozzle if they alight there.

5.8. Beamstops

The position of the beamstop can have a significant effect on the data quality. The beamstop should be aligned properly to avoid asymmetric scattering, as this background will give large values of $R(I)_{\rm sym}$ at low resolution. Most beamstops can be pulled away from the crystal position for easier flash-cooling access. The crystal-to-beamstop distance used for data collection is a compromise between being short, to minimize main beam background from air scatter but causing the loss of low-resolution data, and being long, which gives the low-resolution data but increases the background (see Fig. 9).

On home sources, the background can be significantly reduced by minimizing the collimator-to-beamstop distance, *e.g.* a reduction of 60% was observed when the collimator-to-crystal and the crystal-to-beamstop distances were reduced from 11 to 4 mm and 27 to 7 mm, respectively. If the beamstop shadow on the diffraction image seems too large, it is worth checking the beamstop and collimator end for Plasticene and fluff. Alternatively, the beamstop might be bigger than necessary, and a smaller one could be installed.

6. If nothing seems to work . . .

Occasionally the experimenter is faced with a problem protein crystal, for which an appropriate cryo-solution cannot be found, or having found a seemingly benign cryo-solution, the diffraction is still not satisfactory. In these circumstances, there are various aspects of the cryo-cooling procedure which can be changed in a search for better results. However, it is always worth having more than one attempt at flash-cooling before

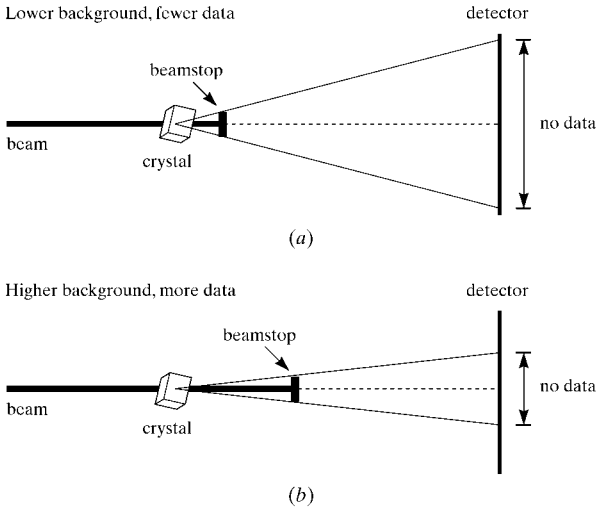

Figure 9
Two extremes of beamstop position. (*a*) Beamstop near the crystal gives low background from main beam scattering from air but obscures the low-resolution diffraction data. (*b*) Beamstop further from the crystal gives higher background but allows more low-resolution data to be recorded. The beamstop position will be a compromise between these two extremes

giving up on a particular set of conditions, as small differences in procedure can often make the difference between success and failure.

Before embarking on any of the experiments suggested below, it is very useful to collect some data from a crystal mounted in a quartz or glass capillary tube at room temperature to give an idea of its intrinsic diffraction power and mosaicity. If there is no diffraction beyond 6 Å or if the crystals are highly mosaic, it is unlikely that cryo-cooling will improve them. Having established, for instance, that the crystals diffract to 3.0 Å on an in-house source at room temperature, it is worth the effort of finding appropriate cryo-conditions.

6.1. Cryo-solutions

If the cryo-solutions have unfortunately been made up by adding cryo-agents to the original mother-liquor stock solution, it is worth making up a more concentrated stock solution of mother liquor and adding cryoprotecting agents to this in such proportions that the original mother-liquor component concentrations remain the same, *i.e.* the cryoprotecting agent replaces water in the mother liquor rather than diluting it. For instance, if the mother liquor has concentration X, make up a $2X$ solution, and to make 100 µl of 5% cryo-solution, mix 50 µl $2X$, 5 µl glycerol and 45 µl water.

As well as the more common cryoprotecting agents already mentioned, others such as erythritol, xylitol, inositol, raffinose, trehalose, 2,3,*R*,*R*-butanediol, propylene glycol, 2-propanol (concentrations up to 70% required), DMSO (dimethyl sulfoxide) and other alcohols have been used successfully. This list is by no means exhaustive and mixtures of two different agents have also been found helpful, as well as treatment with a cryo-solution followed by immersion in oil such as Paratone-N (Kwong & Liu, 1999) prior to flash-cooling. Crystals have also been found to tolerate flash-freezing better after being gently cross-linked with glutaraldehyde (Lusty, 1999).

If no benign cryo-solution can be found, another option is to exchange the mother liquor in the crystals for another solution in which the crystals are stable and which can be more easily cryoprotected. This exchange may have to be performed slowly and/or gradually. A convenient vapour-diffusion method of finding an alternative solvent has been reported by Wierenga *et al.* (1992). If the crystals do not react well to a sudden change of solvent, a flow cell can be used. For instance, in the study of phosphoglucomutase, 2 *M* ammonium sulfate and PEG 3350 was replaced over many hours in a flow cell by PEG 600 (Ray *et al.*, 1997). A decrease in mosaic spread and an improvement of the diffraction limit from 2.75 to 2.35 Å was observed.

6.2. Cryogen choice

The most common cryogens in use are liquid nitrogen [melting point (MP), 63 K; boiling point (BP), 78 K], propane (MP, 86 K; BP, 231 K) and gaseous nitrogen. Measurements of the cooling rates of various cryogens are notoriously difficult to make, because of the heat carried into the system by the measuring instrument. For samples comparable with a typical protein crystal, there are two reported sets of measurements (Teng & Moffat, 1998; Walker *et al.*, 1998). Both concluded that gaseous nitrogen is the slowest in cooling between 300 and 100 K, but were at variance on whether liquid propane or liquid nitrogen was faster overall. The results depend critically on the size of the sample and the cooling regimes (nucleate or film boiling). Teng and Moffatt concluded that gaseous nitrogen provides the fastest cooling rate between 300 and 250 K, propane is fastest between 250 and 150 K and liquid nitrogen fastest between 150 and 80 K. Gaseous helium allows fast (>500 K s^{-1}) cooling over the larger temperature range of 300–15 K.

Generally, the simplest technique is to stream-freeze into gaseous nitrogen. If stream-freezing has failed, both propane and liquid nitrogen are worth a try. Note that there are safety implications of using propane in the laboratory and some problems may be experienced in shipping dry dewars with crystals frozen in propane to synchrotrons. More experimenters are now also trying ethane as a cryogen, and freon 12 and methylcyclopentane have also been used.

6.3. Transfer/handling/soaking procedures

Some protein crystals are very sensitive to any handling, and the way the cryoprotectant agent is introduced can also have a great impact on the observed diffraction pattern. As a general rule, handling should be minimized. It is worth thinking about the way the crystals are treated from the moment of opening up the tray in which they were grown to the point they are flash-cooled, and considering all the stages where degradation of crystal order might occur. For manipulation of crystals, acupuncture needles are extremely useful and are also cheap. Loops can be used to move crystals gently from the growing drop to the soaking well. In sequential soaks, crystals are better not moved between soaking wells (see §5.3).

Another variable which can be explored is the temperature of the cryo-solution soak. Some experimenters routinely leave their crystals in cryo-solutions overnight at 277 K prior to flash-cooling.

A critical step in the cryo-cooling procedure is the time taken to transfer the crystal from the soaking drop to the cryogen: this should be as swift as possible. If stream-freezing straight onto the goniostat, it is advisable to block the stream with a narrow piece of card until the crystal is safely positioned in the pre-centered place and the transfer tweezers are well out of the way. The card is then quickly removed. This prevents inadvertent knocking of the crystal out of the stream after it has been frozen.

6.4. Osmolarity matching

When they are soaked in cryo-solutions, crystals often suffer from a large osmotic shock and are thus compressed, resulting in cracks, mosaic spread increase and resolution degradation. One approach to overcome this is to match the osmolarity (Os l^{-1}) or osmality (Os kg^{-1}) of the mother liquor (or stabilizing solution) and cryo-solution by modifying the

concentration of the stabilizing solution. Osmalities are tabulated for most of the commonly used solutions in Section D of the *Handbook of Chemistry and Physics* (1988–1989; full editions only). So, for example (David, 1999), for a protein crystal grown in 2.0 *M* NaCl and 50 m*M* pH 7.8 Tris–HCl, the osmality is 3.95 Os kg^{-1}. The mother liquor requires the addition of 20% glycerol for adequate cryo-protection; 20% glycerol (~2.27 g mol l^{-1}) has an osmality of 2.9 Os kg^{-1}. The difference in osmality between the glycerol and mother liquor is 1.05 Os kg^{-1}, so in order to match the osmalities, the new stabilizing solution must have an osmality of 1.05 Os kg^{-1}, which is equivalent to 0.55 *M* NaCl. The crystal may thus be stable in a 20% glycerol/0.55 *M* NaCl solution which has the same osmality as 2.0 *M* NaCl, whereas it was damaged by a 20% glycerol/2 *M* NaCl solution. Lower salt concentration solutions require a higher percentage of cryo-agent for cryo-protection than higher molar salt solutions, so it may be that in this example the glycerol concentration would have to be increased a little to compensate for the removal of salt. The new stabilizing buffer can be introduced through vapour equilibration overnight (for example, using the method of David & Burley, 1991) and the crystal then soaked in the new cryo-solution prior to flash-cooling.

6.5. Crystal annealing

Some researchers have had success in extending the diffraction limits and decreasing the mosaicity of their crystals by the technique of crystal annealing, where the frozen sample is allowed to thaw to room temperature and is then flash-cooled again, sometimes being cycled in this way several times. Two methods of cycling have been reported. In one (Yeh & Hol, 1998), the crystal was rapidly thawed and re-frozen *in situ* on the goniostat by blocking the gas stream for 1.5–2 s and waiting 6 s before repeating the process twice more. In the other (Harp *et al.*, 1998, 1999), the frozen crystals were removed from the goniostat and replaced into the cryo-solution for at least 3 min before being frozen again.

It is possible that the static disorder of the crystals is reduced during the annealing procedure. Crystal annealing is always worth trying, although as with many aspects of work with protein crystals, it does not necessarily succeed in all cases.

7. Future development of cryo-techniques

Can further advances in cryo-techniques help us overcome radiation damage to macromolecular crystals in third-generation synchrotron wiggler- and undulator-produced beams?

Consideration of the energy loss of electrons in samples being investigated by electron microscopy compared with the energy loss of 8 keV X-rays has allowed a theoretical estimate of the maximum X-radiation dose a protein crystal held at 80 K might be able to tolerate (Henderson, 1990). This dose, of around 1.2×10^{17} keV mm^{-3} (2×10^{7} Gray, 1.6×10^{16} photons mm^{-2}), corresponds to approximately 5 years on a rotating anode and 24 h on a second-generation synchrotron wiggler beamline; significantly less on a third-generation undulator source. Gonzales & Nave (1994) tested this prediction for lysozyme crystals held at 100 K and observed radiation damage at a dose in good agreement with that calculated by Henderson. A detailed discussion of the physical factors which are thought to be pertinent to radiation damage in protein crystals can be found in Nave (1995).

For a crystal held at around 100 K, the energy density per unit volume at low photon flux is probably not high enough to induce significant heating effects. In extremely bright beams, the energy density per unit volume will produce enough thermal energy to literally vapourize samples even at 100 K, as has been observed in some third-generation synchrotron beams. It follows that there is a threshold energy density where damage arising from local heating becomes appreciable. This threshold will vary mostly with crystal surface-to-volume ratio and local cooling regimes. Although the primary damage is largely unavoidable and inescapable, a small proportion may not be, and there are several possible ways by which the overall radiation damage caused by high-intensity beams might be reduced.

7.1. Data-collection rate

As yet, there has been little systematic study of the relationship between beam heating of the sample and radiation damage. Experiments which monitored the rate of radiation damage inflicted by a white beam on line 9.5 at SRS Daresbury for different incident fluxes (Gonzales & Nave, 1994) seemed to indicate that the sample degradation was not a consequence of beam heating, but rather to primary damage, although this result has not been confirmed for more intense or for monochromatic beams.

Sample heating will undoubtedly occur in very intense beams, and there may be some advantage in collecting data at less than the maximum possible rate (attenuated flux and/or pulsed beam and/or short exposures followed by beam-off sample 'resting' time), since beam heating averaged over time should then be reduced and this should lessen the degradation rate. Collecting the data at a higher rate will only reduce the speed of radiation damage if the time component of the damage is significant. With CCD-based detectors, detector read-out time is much reduced and is no longer so significant a factor. Data can be collected so quickly with the high available fluxes that secondary damage should be low. For instance, a MAD experiment performed recently at the APS took only 23 min for four wavelengths (16 kDa protein, CCD-based detector, 3 s per image with 2° oscillation, space group $C222_1$, unit-cell dimensions 62.7, 64.7 and 74.2 Å, resolution 2.25 Å, 60 images per data set, 5 min 45 s per data set; Walsh *et al.*, 1999). For this experiment, the APS beam was attenuated by a factor of ten with an aluminium filter and defocused from 200 × 200 µm to 600 × 600 µm. Thus, potentially the flux could have been at least 100 times higher (assuming a square beam-intensity distribution). If the sample could have withstood this flux, the exposure time per image could have been much

shorter and the experiment could have been completed in an even shorter time. For very fast data collection, high-speed and high-precision goniometer motors are required.

7.2. Change the incident X-ray wavelength

Experimentally, there is much anecdotal evidence that at room temperature more data can usually be obtained from the same protein crystal at lower X-ray wavelengths, where beam absorption is decreased. Helliwell (1992) has performed model calculations for room-temperature samples using X-ray wavelengths down to 0.33 Å, which suggest that the amount of data recorded per crystal will increase as the wavelength is reduced.

Changing the wavelength influences the primary radiation damage, but the nature of the relationship is not yet known. Radiation damage may increase with the amount of energy absorbed per scattered photon or (possibly and) with the number of quanta absorbed. Arndt (1984) has shown that when transmission through the crystal is high, the energy absorbed per scattered photon is almost independent of wavelength, which implies that if energy absorption is the more important factor for radiation damage, there will be only a small advantage in collecting data at shorter wavelengths. Experimentally, Gonzales & Nave (1994), using different thickness absorbers in a white beam, concluded that there was no reduction in radiation damage to a 100 K crystal at shorter wavelengths, but these experiments need to be repeated with monochromatic beams.

7.3. Go to lower cryogen temperatures

A commercially available open-flow cryostat now allows the possibility of data collection at temperatures down to 28 K (HeliX, Oxford Cryosystems, Long Hanborough, Oxon). To consider whether the gain of going to lower cryogen temperature outweighs the disadvantages (mainly cost), some of the factors which might be relevant are outlined below.

7.3.1. Thermal conductivity, k, and specific heat, C_p, of helium compared with those of nitrogen. Both the thermal conductivity and the specific heat of the cryogen affect, along with many other parameters, the heat-exchange coefficient. The flow regime of open-flow cryostats is laminar: any turbulence around the crystal position will assist heat transfer. The thermal conductivity, k, of helium at 30 K is 0.35 mW cm^{-1} K^{-1}, whereas for nitrogen at 100 K, k is 0.1 mW cm^{-1} K^{-1}. The specific heat of helium is also a little higher than that of nitrogen (5.2 J g m^{-1} K^{-1} for helium compared with 1.25 J g m^{-1} K^{-1} for nitrogen; mass ratio He:N is 4:14) so more heat can be carried away by the same unit mass (at 30 K the gas is denser, so care must be taken in comparing flow rates, velocities, masses and volumes of helium and nitrogen at different temperatures). Helium at 30 K should therefore be a more efficient cryogen than nitrogen gas at 100 K, and this is borne out by experience in that cold-burns are much more swiftly inflicted by helium-gas streams than by nitrogen-gas streams held at the same temperature.

Table 1
Enhancement in reflection intensities for ribonuclease A.

d (Å)	I_{98}/I_{300}	I_{30}/I_{300}
3.0	1.5	1.6
2.0	2.5	2.9
1.0	40	61

7.3.2. Reduction of thermal vibration and thus atomic B factor at lower temperature. As the temperature of a protein molecule is decreased from 293 K, the dynamic disorder decreases, until below around 150 K all that remains is the zero-point motion (theoretical limit at 0 K), the Debye-solid harmonics and the static disorder. Of these, only the Debye-solid harmonics will decrease as the temperature is lowered further, and so the reduction of atomic B factors, in going from 100 to 30 K is likely to be fairly small.

However, any reduction in B factor with decreasing temperature effectively enhances the intensity of the data in all resolution ranges, with an increasing effect as the resolution increases, since the intensity I is given by

$$I \propto \exp(-2B/4d^2), \qquad (1)$$

where d is the resolution of the data in Å and B is the atomic B factor in Å^2. What can we learn about the effect of the B-factor reduction with decreasing temperature for proteins where experimental average B factors are known?

Tilton *et al.* (1992), for instance, give the average B factors at different temperatures for ribonuclease A, a 124 amino-acid predominantly β-sheet protein. The dependence of B on temperature for this protein appears to be biphasic, increasing by 1.2 Å^2 per 100 K up to 200 K and by 6.4 Å^2 per 100 K above 200 K. Specific values of $\langle B\rangle_T$ are $\langle B\rangle_{300}$ = 14 Å^2 (measured), $\langle B\rangle_{98}$ = 6.6 Å^2 (measured) and $\langle B\rangle_{30}$ = 5.8 Å^2 (extrapolated). The enhancements in reflection intensities at different resolutions and temperatures can be calculated using (1) and are shown in Table 1.

For a larger protein, we can carry out similar calculations from the data of Fülöp *et al.* (1995) on cytochrome cd_1 nitrite reductase, which has 2 × 567 amino acids in the asymmetric unit. Average B values for the protein at different temperatures are $\langle B\rangle_{300}$ = 16 Å^2 (measured), $\langle B\rangle_{98}$ = 13.2 Å^2 (measured) and $\langle B\rangle_{30}$ = 12.2 Å^2 (extrapolated). Table 2 shows the resulting relative intensity ratios.

The predicted enhancement is most significant at higher resolutions and is ten times smaller for the nitrite reductase compared with the ribonuclease A. Thus, the intensity-enhancement effect of the lower B factors is only likely to be significant for data beyond 1.5 Å and for smallish proteins. Since most structural studies are carried out at between 2 and 3 Å resolution, this implies that enhancement of B factor is likely to give only a marginal advantage for samples at 30 K as compared with 100 K.

However, the lower B factors effectively reduce the dynamic range of the data, which for high-resolution data collections might mean that fewer data-collection passes are

Table 2
Enhancement in reflection intensities for cytochrome cd_1 nitrite reductase.

d (Å)	I_{100}/I_{300}	I_{30}/I_{300}
3.0	1.2	1.24
2.0	1.4	1.6
1.0	4.1	6.8

necessary, thus enabling the experiment to be completed in a shorter time.

7.3.3. Temperature-dependence of the thermal conductivity, *k*, of crystals. The temperature-dependence of k has not been measured for protein crystals in vitreous ice, but the thermal conductivity may become very low at low temperatures. For glasses, and also for clathrate hydrates (maximum 6 Å diameter molecules trapped in a matrix of ice) where measurements are available down to 100 K (Ross & Andersson, 1982; Andersson & Ross, 1983), $k \propto T$. For perfect crystalline solids, $k \propto 1/T$. Protein crystals are likely to mimic the clathrates rather than perfect crystals and will thus have $k \propto T$. The rate of heat conduction with time is

$$(\mathrm{d}Q/\mathrm{d}T) = kA(\mathrm{d}T/\mathrm{d}x),$$

where Q is the heat in J, t is the time in s, A is the cross-sectional area in m^2, T is the temperature and x is the distance across the temperature gradient in m. Thus, if k becomes very small, the heat-transfer rate ($\mathrm{d}Q/\mathrm{d}t$) from the centre of the sample to the cryogen also decreases.

7.3.4. Temperature-dependence of specific heat capacity, C_p, of crystals. This parameter is similarly not yet measured for protein crystals, but there is reason to think it may also become very low at low temperatures. Measurements for vitreous glass and various different vitrified salt solutions all show a decrease in C_p with decreasing temperature (Angell & Tucker, 1980). The heat, H, required to raise the temperature of a mass m by ΔT is

$$H = mC_p\Delta T.$$

Thus, at lower temperature less energy is needed to heat the crystal and the thermal conductivity may also be lower, so it will be harder to conduct the heat away by cooling. Although counter-intuitive, the effect of this will be that the centre of the crystal will heat up faster and be harder to cool when held at 30 K compared with 100 K. However, it will still be advantageous to hold the crystal at 30 K, as the time taken to heat the centre up to 100 K will be gained. The equilibrium heat-transfer state for a crystal at 30 K should allow a higher incident energy flux for the same level of beam heating.

7.3.5. Temperature-dependence of primary radiation damage. The temperature-dependence of primary radiation damage will depend on the (as yet unknown) temperature dependence of the density of colour centres, crystal defects, shrinkage and crystal contact changes owing to cell shrinkage with decreasing temperature. This list is not exhaustive and, because the mechanism of radiation damage itself is poorly understood, there may be additional factors which will affect the balance of advantage/disadvantage in going to lower cryogen temperature.

7.3.6. Cooling regime. For the actual flash-cooling procedure, there is advantage in cooling the sample down to lower temperatures. Newton's Law of Cooling states that $\mathrm{d}T/\mathrm{d}t$ is proportional to ΔT. ΔT between room temperature and 100 K gaseous nitrogen is approximately 193 K (ΔT_1) and is 263 K (ΔT_2) for helium cooling running at 30 K. Thus $\Delta T_2/\Delta T_1 = 1.4$. Teng & Moffat (1998) reported that at 20 K and a helium flow rate of 40 l min^{-1}, a cooling rate of >500 K s^{-1} was achieved in the temperature range 300–150 K and a rate of <100 K s^{-1} was achieved in the temperature range 120–20 K. The lower helium temperature and the heat-transfer properties of helium must thus surely be an advantage in providing a more efficient cooling regime. Although this does not directly impact the rate of radiation damage during data collection, it does decrease the amount of cryoprotectant agent required to obtain a vitreous glass. The relationship between the rate of radiation damage for different cryo-solution concentrations has not yet been investigated and is therefore another uncertainty when considering damage avoidance.

8. Conclusions

From the above discussion, it can be seen that there are too many simultaneous variables to make a prediction of whether using helium as a cryogen will be effective in reducing radiation damage inflicted by very hot beams. The answer will depend on the balance of advantages and disadvantages outlined above.

Since heat removal from the sample is proportional to its surface area and heat deposition by the beam is proportional to the sample volume, the surface-to-volume ratio of the crystal may well be the most important single parameter in tipping the balance of advantage/disadvantage of reducing the temperature to 30 K. Therefore, larger S/V crystals can be used with more brilliant beams to improve the heat-transfer properties. Smaller crystals overall can be used productively since the flux is so large, but there will always be a lower limit to the crystal size owing to primary radiation damage (Gonzales & Nave, 1994). It is vital for us to acquire a better understanding of the interplay between the various experimental parameters and, in particular, the radiation-damage process itself before any conclusions can be drawn. Systematic experiments, balancing cost with likely gain, are required over the next few years to enable us to optimize the use of the X-ray beams now available to the macromolecular crystallography community.

I would like to thank all the various people with whom I have discussed data collection, cryo-techniques and radiation damage at courses and meetings, as well as my past and present colleagues at the LMB, Oxford. I am especially grateful for input from Thomas Schneider, Martin Noble,

Peter David, John Cosier, Peter Kuhn, Susan Lea and Colin Nave. I thank Stephen Lee for assistance with the figures. This work is supported by the UK Medical Research Council.

References

Andersson, P. & Ross, R. (1983). *J. Phys. C Solid State Phys.* **16**, 1423–1432.

Angell, C. A. & Tucker, J. C. (1980). *J. Phys. Chem.* **84**, 268–272.

Arndt, U. (1984). *J. Appl. Cryst.* **17**, 118–119.

Brown, N., Noble, M. E. M., Endicott, J. A., Garman, E. F., Wakatsuki, S., Mitchell, E., Rasmussen, B., Hunt, T. & Johnson, L. N. (1995). *Structure*, **3**, 1235–1247.

Dauter, Z. (1997). *Methods Enzymol.* **276**, 326–344.

David, P. R. (1999). In *Practical Protein Crystallography*, edited by D. McRee, 2nd ed. New York: Academic Press.

David, P. R. & Burley, S. K. (1991). *J. Appl. Cryst.* **24**, 1073–1074.

Esnouf, R. M., Ren, J., Garman, E. F., Somers, D. O'N., Ross, C. K., Jones, E. Y., Stammers, D. K. & Stuart, D. I. (1998). *Acta Cryst.* D**54**, 938–953.

Fülöp, V., Moir, J. W. B., Ferguson, S. J. & Hadju, J. (1995). *Cell*, **81**, 369–377.

Gamblin, S. J. & Rodgers, D. W. (1993). *Proceedings of the CCP4 Study Weekend. Data Collection and Processing*, edited by L. Sawyer, N. Isaacs & S. Bailey, pp. 28–32. Warrington: Daresbury Laboratory.

Garman, E. F. (1993). *Proceedings of the CCP4 Study Weekend. Data Collection and Processing*, edited by L. Sawyer, N. Isaacs & S. Bailey, pp. 123–131. Warrington: Daresbury Laboratory.

Garman, E. F. (1999). *Protein Crystallization: Techniques, Strategies, and Tips. A Laboratory Manual*, edited by T. Bergfors, ch. 17. La Jolla, California: International University Line.

Garman, E. F. & Mitchell, E. P. (1996). *J. Appl. Cryst.* **29**, 584–587.

Garman, E. F. & Schneider, T. R. (1997). *J. Appl. Cryst.* **30**, 211–237.

Garman, E. F., Wouters, J., Vimr, E., Laver, G. & Sheldrick, G. M. (1996). *Acta Cryst.* A**52**, C8.

Gonzales, A. & Nave, C. (1994). *Acta Cryst.* D**50**, 874–877.

Gregoriou, M., Noble, M. E. M., Watson, K. A., Garman, E. F., Krulle, T. M., de la Fuente, C., Fleet, G. W. J., Oikonomakos, N. K. & Johnson, L. N. (1998). *Protein Sci.* **7**, 915–927.

Haas, D. J. & Rossmann, M. G. (1970). *Acta Cryst.* B**26**, 998–1004.

Handbook of Chemistry and Physics (1988–1989). 69th ed., edited by R. C. Weast, Table D-232. Boca Raton, Florida: CRC Press.

Harp, J. M., Leif Hanson, B., Timm, D. E. & Bunick, G. J. (1999). *Acta Cryst.* D**55**, 1129–1334.

Harp, J. M., Timm, D. E. & Bunick, G. J. (1998). *Acta Cryst.* D**54**, 622–628.

Helliwell, J. R. (1992). *Macromolecular Crystallography with Synchrotron Radiation.* Cambridge University Press.

Henderson, R. (1990). *Proc. R. Soc. Lond. B*, **241**, 6–8.

Hope, H. (1988). *Acta Cryst.* B**44**, 22–26.

Kabsch, W. (1988). *J. Appl. Cryst.* **21**, 916–924.

Kwong, P. D. & Liu, Y. (1999). *J. Appl. Cryst.* **32**, 102–105.

Leslie. A. G. W. (1996). *CCP4 Newslett. Protein Crystallogr.* **32**, 7–8.

Low, B. W., Chen, C. C. H., Berger, J. E., Singman, L. & Pletcher, J. F. (1966). *Proc. Natl Acad. Sci. USA*, **56**, 1746–1750.

Lusty, C. J. (1999). *J. Appl. Cryst.* **32**, 106–112.

Messerschmidt, A. & Pflugrath, J. W. (1987). *J. Appl. Cryst.* **20**, 306–315.

Mitchell, E. P. & Garman, E. F. (1994). *J. Appl. Cryst.* **27**, 1070–1074.

Mitchell, E. P., Kuhn, P. & Garman, E. F. (1999). *Structure*, **7**, R111–R121.

Nagata, C., Moriyama, H., Tanaka, N., Nakasako, M., Yamamoto, M., Ueki, T. & Oshima, T. (1996). *Acta Cryst.* D**52**, 623–630.

Nave, C. (1995). *Radiat. Phys. Chem.* **45**, 483–490.

Noble, M. E. M. (1996). *PREDICT Package*, http://biop.ox.ac.uk/www/distrib/predict.html.

Otwinowski, Z. & Minor, W. (1997). *Methods Enzymol.* **276**, 307–326.

Parkin, S. & Hope, H. (1998). *J. Appl. Cryst.* **31**, 945–953.

Ravelli, R. G. B., Sweet, R. M., Skinner, J. M., Duisenberg, A. J. M. & Kroon, J. (1997). *J. Appl. Cryst.* **30**, 551–554.

Ray, W. R. Jr, Baranidharan, S. & Liu, Y. (1997). *Acta Cryst.* D**53**, 385–391.

Rodgers, D. (1997). *Methods Enzymol.* **276**, 183–203.

Ross, R. & Andersson, P. (1982). *Can. J. Phys.* **60**, 881–892.

Sauer, O., Schmidt, A. & Kratky, C. (1997). *J. Appl. Cryst.* **30**, 476–486.

Schick, B. & Jurnak, F. (1994). *Acta Cryst.* D**50**, 563–568.

Smith, J. L. (1991). *Curr. Opin. Struct. Biol.* **1**, 1002–10011.

Soltis, S. M., Stowell, M. H. B., Wiener, M. C., Philips, G. N. & Rees, D. C. (1997). *J. Appl. Cryst.* **30**, 190–194.

Teng, T.-Y. (1990). *J. Appl. Cryst.* **23**, 387–391.

Teng, T.-Y. & Moffat, K. (1998). *J. Appl. Cryst.* **31**, 252–257.

Tilton, R. F. Jr, Dewan, J. & Petsko, G. A. (1992). *Biochemistry*, **31**, 2469–2481.

Tsitsanou, K. E., Oikonomakos, N. G., Zogrphos, S. E., Skamnaki, V. T., Gregoriou, M., Watson, K. A., Johnson, L. N. & Fleet, G. W. J. (1999). *Protein Sci.* **8**, 741–749.

Walker, L. J., Moreno, P. O. & Hope, H. (1998). *J. Appl. Cryst.* **31**, 954–956.

Walsh, M. A., Dementieva, I., Evans, G., Sanishvili, R. & Joachimiak, A. (1999). *Acta Cryst.* D**55**, 1168–1173.

Wierenga, R. K. Zeelan, J. P. & Noble, M. E. M. (1992). *J. Cryst. Growth.* **122**, 231–234.

Yeh, J. I. & Hol, W. G. J. (1998). *Acta Cryst.* D**54**, 479–480.